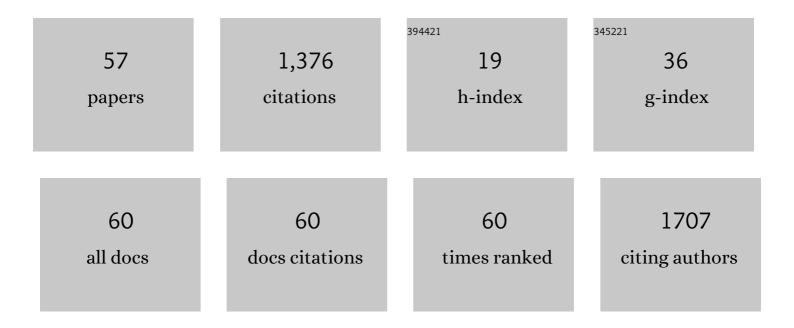
Damian Kowalski

List of Publications by Year in descending order

Source: https://exaly.com/author-pdf/4896027/publications.pdf Version: 2024-02-01



DAMIAN KOWALSKI

#	Article	IF	CITATIONS
1	TiO2 nanotubes, nanochannels and mesosponge: Self-organized formation and applications. Nano Today, 2013, 8, 235-264.	11.9	324
2	Self-healing ion-permselective conducting polymer coating. Journal of Materials Chemistry, 2010, 20, 7630.	6.7	96
3	Corrosion protection of steel by bi-layered polypyrrole doped with molybdophosphate and naphthalenedisulfonate anions. Corrosion Science, 2007, 49, 1635-1644.	6.6	72
4	Polypyrrole self-organized nanopore arrays formed by controlled electropolymerization in TiO2 nanotube template. Chemical Communications, 2010, 46, 8585.	4.1	62
5	The effect of ultrasonic irradiation during electropolymerization of polypyrrole on corrosion prevention of the coated steel. Corrosion Science, 2008, 50, 286-291.	6.6	55
6	Brownmilleriteâ€ŧype Ca ₂ FeCoO ₅ as a Practicable Oxygen Evolution Reaction Catalyst. ChemSusChem, 2017, 10, 2864-2868.	6.8	50
7	The effect of counter anions on corrosion resistance of steel covered by bi-layered polypyrrole film. Corrosion Science, 2007, 49, 3442-3452.	6.6	44
8	Polymer nanowires or nanopores? Site selective filling of titania nanotubes with polypyrrole. Journal of Materials Chemistry, 2011, 21, 17909.	6.7	44
9	Electrochemical synthesis of 1D core-shell Si/TiO2 nanotubes for lithium ion batteries. Journal of Power Sources, 2017, 361, 243-248.	7.8	39
10	On the mechanism of photocatalytic reactions on Cu _x O@TiO ₂ core–shell photocatalysts. Journal of Materials Chemistry A, 2021, 9, 10135-10145.	10.3	35
11	Current dependent formation of PEDOT inverse nanotube arrays. RSC Advances, 2013, 3, 2154.	3.6	32
12	Highâ€Efficiency Direct Ammonia Fuel Cells Based on BaZr _{0.1} Ce _{0.7} Y _{0.2} O _{3â^`} <i>_δ</i> /Pd Oxideâ€Metal Junctions. Global Challenges, 2018, 2, 1700088.	3.6	25
13	Activation of Catalytically Active Edge-Sharing Domains in Ca ₂ FeCoO ₅ for Oxygen Evolution Reaction in Highly Alkaline Media. ACS Applied Materials & Interfaces, 2019, 11, 28823-28829.	8.0	25
14	<i>In Situ</i> Activation of a Manganese Perovskite Oxygen Reduction Catalyst in Concentrated Alkaline Media. Journal of the American Chemical Society, 2021, 143, 6505-6515.	13.7	25
15	Bi2WO6â€based Z-scheme photocatalysts: Principles, mechanisms and photocatalytic applications. Journal of Environmental Chemical Engineering, 2022, 10, 107838.	6.7	24
16	Advanced Geometries of PEDOT Formed in Titania Nanotubes. ChemPhysChem, 2012, 13, 3790-3793.	2.1	23
17	In Situ Activation of Anodized Ni–Fe Alloys for the Oxygen Evolution Reaction in Alkaline Media. ACS Applied Energy Materials, 2020, 3, 12316-12326.	5.1	23
18	Long-term durability of platelet-type carbon nanofibers for OER and ORR in highly alkaline media. Applied Catalysis A: General, 2020, 597, 117555.	4.3	23

#	Article	IF	CITATIONS
19	Low electric field strength self-organization of anodic TiO2 nanotubes in diethylene glycol electrolyte. Journal of Materials Chemistry A, 2015, 3, 6655-6661.	10.3	22
20	La _{0.7} Sr _{0.3} Mn _{1–<i>x</i>} Ni _{<i>x</i>} O _{3â~îî} Elector for the Four-Electron Oxygen Reduction Reaction in Concentrated Alkaline Media. Journal of Physical Chemistry C, 2018, 122, 22301-22308.	ctrocatalys 3.1	sts 20
21	Slippery Liquid-Infused Porous Surfaces on Aluminum for Corrosion Protection with Improved Self-Healing Ability. ACS Applied Materials & amp; Interfaces, 2021, 13, 45089-45096.	8.0	20
22	Ex Situ Evidence for the Role of a Fluorideâ€Rich Layer Switching the Growth of Nanopores to Nanotubes: A Missing Piece of the Anodizing Puzzle. ChemElectroChem, 2018, 5, 610-618.	3.4	19
23	Fabrication of superhydrophobic copper metal nanowire surfaces with high thermal conductivity. Applied Surface Science, 2021, 537, 147854.	6.1	17
24	High strength hydrogels enable dendrite-free Zn metal anodes and high-capacity Zn–MnO ₂ batteries <i>via</i> a modified mechanical suppression effect. Journal of Materials Chemistry A, 2022, 10, 3122-3133.	10.3	17
25	High Proton Conductivity in Anodic ZrO ₂ /WO ₃ Nanofilms. Angewandte Chemie - International Edition, 2009, 48, 7582-7585.	13.8	16
26	Enhanced hydrogen permeability of hafnium nitride nanocrystalline membranes by interfacial hydride conduction. Journal of Materials Chemistry A, 2018, 6, 2730-2741.	10.3	16
27	Highly Active and Durable FeNiCo Oxyhydroxide Oxygen Evolution Reaction Electrocatalysts Derived from Fluoride Precursors. ACS Sustainable Chemistry and Engineering, 2021, 9, 9465-9473.	6.7	16
28	Self-organization of TiO2 nanotubes in mono-, di- and tri-ethylene glycol electrolytes. Electrochimica Acta, 2016, 204, 287-293.	5.2	15
29	A lithiophilic carbon scroll as a Li metal host with low tortuosity design and "Dead Li―self-cleaning capability. Journal of Materials Chemistry A, 2021, 9, 13332-13343.	10.3	15
30	Role of electrochemical process parameters on the electrodeposition of silicon from 1-butyl-1-methylpyrrolidinium bis(trifluoromethanesulfonyl)imide ionic liquid. Electrochimica Acta, 2018, 265, 166-174.	5.2	14
31	Flow-Injection Preconcentration of Chloramphenicol Using Molecularly Imprinted Polymer for HPLC Determination in Environmental Samples. Journal of Automated Methods and Management in Chemistry, 2011, 2011, 1-10.	0.5	13
32	Electrocatalytic and Photoelectrochemical Reduction of Carbon Dioxide at Hierarchical Hybrid Films of Copper(I) Oxide Decorated with Tungsten(VI) Oxide Nanowires. Journal of the Electrochemical Society, 2019, 166, H3271-H3278.	2.9	13
33	Self-healing Ability of Conductive Polypyrrole Coating with Artificial Defect. ECS Transactions, 2009, 16, 177-181.	0.5	12
34	Fabrication of Superoleophobic Surface on Stainless Steel by Hierarchical Surface Roughening and Organic Coating. ISIJ International, 2019, 59, 345-350.	1.4	12
35	A low-cost and non-corrosive electropolishing strategy for long-life zinc metal anode in rechargeable aqueous battery. Energy Storage Materials, 2022, 46, 223-232.	18.0	12
36	Fluorineâ€Free Slippery Liquidâ€Infused Porous Surfaces Prepared Using Hierarchically Porous Aluminum. Physica Status Solidi (A) Applications and Materials Science, 2020, 217, 1900836.	1.8	10

Damian Kowalski

#	Article	IF	CITATIONS
37	Highly Durable Oxygen Evolution Reaction Catalyst: Amorphous Oxyhydroxide Derived from Brownmillerite-Type Ca ₂ FeCoO ₅ . ACS Applied Energy Materials, 2020, 3, 5269-5276.	5.1	10
38	High dispersion and oxygen reduction reaction activity of Co ₃ O ₄ nanoparticles on platelet-type carbon nanofibers. RSC Advances, 2019, 9, 3726-3733.	3.6	9
39	Incorporation and migration of phosphorus species within anodic films on an Alâ€W alloy. Surface and Interface Analysis, 2011, 43, 893-902.	1.8	8
40	High-corrosion-resistance mechanism of graphitized platelet-type carbon nanofibers in the OER in a concentrated alkaline electrolyte. Journal of Materials Chemistry A, 2022, 10, 8208-8217.	10.3	8
41	Brownmillerite-type Ca2 FeCoO5 as a Practicable Oxygen Evolution Reaction Catalyst. ChemSusChem, 2017, 10, 2841-2841.	6.8	5
42	Ultra-rapid formation of crystalline anatase TiO2 films highly doped with substrate species by a cathodic deposition method. Electrochemistry Communications, 2019, 108, 106561.	4.7	5
43	Characterization of Dark-Colored Nanoporous Anodic Films on Zinc. Coatings, 2020, 10, 1014.	2.6	5
44	Spinel-Type Metal Oxide Nanoparticles Supported on Platelet-Type Carbon Nanofibers as a Bifunctional Catalyst for Oxygen Evolution Reaction and Oxygen Reduction Reaction. Electrochemistry, 2020, 88, 566-573.	1.4	5
45	Highly increased breakdown potential of anodic films on aluminum using a sealed porous layer. Journal of Solid State Electrochemistry, 2018, 22, 2073-2081.	2.5	4
46	The role of tungsten species in the transition of anodic nanopores to nanotubes formed on iron alloyed with tungsten. Electrochimica Acta, 2019, 309, 274-282.	5.2	4
47	Compositional variations in anodic nanotubes/nanopores formed on Fe 100, 110 and 111 single crystals. Electrochimica Acta, 2020, 364, 137316.	5.2	4
48	Formation of quasi-spherical Au48-198 clusters in anodic titania nanotubes grown on Ti-Au alloys. Electrochemistry Communications, 2020, 120, 106847.	4.7	3
49	Characterization of Amorphous Anodic Nb2O5 Nanofilm for Gas Sensing. ECS Transactions, 2009, 16, 57-65.	0.5	2
50	Site-Selective Au ⁺ Electroreduction in Titania Nanotubes for Electrochemical and Plasmonic Applications. ACS Applied Nano Materials, 2022, 5, 7696-7703.	5.0	2
51	Exâ€Situ Evidence for the Role of a Fluoride-Rich Layer Switching the Growth of Nanopores to Nanotubes: A Missing Piece of the Anodizing Puzzle. ChemElectroChem, 2018, 5, 570-570.	3.4	1
52	TiO2 Nanotubes As a Matrice for Electrodeposited Si, Au, and CdSe. ECS Meeting Abstracts, 2017, , .	0.0	1
53	1D Core-Shell Nanostructures Formed By Electrodeposition of Metals and Metalloids in Anodic TiO2 Nanotubes. ECS Meeting Abstracts, 2017, , .	0.0	0
54	Ex-Situ Evidence on the Transition of Anodic Nanopores into Nanotubes Formed on Iron. ECS Meeting Abstracts, 2018, , .	0.0	0

#	Article	IF	CITATIONS
55	(Invited) Highly Durable Platelet-Type Carbon Nanofibers for Oer in Alkaline Electrolyte. ECS Meeting Abstracts, 2020, MA2020-01, 2805-2805.	0.0	Ο
56	Spinel-Type Metal Oxide Nanoparticles Supported on Platelet-Type Carbon Nanofibers for Oxygen Evolution Reaction and Oxygen Reduction Reaction. ECS Meeting Abstracts, 2020, MA2020-02, 3618-3618.	0.0	0
57	The Role of Hydrated Alumina Layer on the Incorporation of Electrolyte Species in Anodizing of Aluminum. ECS Meeting Abstracts, 2020, MA2020-02, 1233-1233.	0.0	ο